



ACETYLCHOLINESTERASE, TYROSINASE AND PEROXIREDOXIN ENZYME INHIBITORY ACTIVITY STUDIES OF SYNTHESISED OXADIAZOLES AND THIADIAZOLES FROM SCHIFF BASES

Keerthan, Sindhu T. J., Jainey P. James*, Zakiya Fathima C

Department of Pharmaceutical Chemistry, Nitte (Deemed to be University), NGSM Institute of Pharmaceutical Sciences (NGSMIPS), Deralakatte, Mangaluru-575018, Karnataka, India

With the increasing prevalence of neurodegenerative diseases (NDDs) and the limited effectiveness of existing treatments, there is a pressing need to discover new therapeutic leads that can interact with multiple targets implicated in NDD pathogenesis. A novel series of 1,3,4-oxadiazol-2-amine and 1,3,4-thiadiazol-2-amine derivatives has been designed to evaluate the inhibitory potential of these compounds against acetylcholinesterase, tyrosinase, and peroxiredoxins was tested using *in silico* and *in vitro* methods. Oxadiazole (4a, 4d) and thiadiazole (4e, 4g, 4h) derivatives were synthesised by cyclisation of schiff base using FeCl_3 , further characterised by FTIR, ^1H NMR and mass spectra. *In vitro* inhibitory studies evaluated acetylcholinesterase, tyrosinase and peroxiredoxins enzymes. Molecular docking revealed that compounds 4a and 4e effectively interacted against acetylcholinesterase and tyrosinase. *In vitro* results showed that compounds 4a and 4e exhibited the highest inhibitory activity against acetylcholinesterase and tyrosinase and were good antioxidant agents. The docking results correlated with *in vitro* results confirmed that compound 4a from the oxadiazole series and compound 4e from the thiadiazole series had the most potent acetylcholinesterase and tyrosinase inhibitory activity. Further analysis suggested that heterocyclic groups might be a reason for better acetylcholinesterase and tyrosinase inhibitory action. This indicates additional scope for these derivatives to be explored further as a neuroprotective agent for a better understanding of the underlying mechanisms and pathophysiology.

Keywords: oxadiazole, thiadiazole, acetylcholinesterase, tyrosinase, peroxiredoxins

INTRODUCTION

Neurodegenerative conditions, such as Alzheimer's disease, Parkinson's disease, and Huntington's disease, involve the deterioration of neurons, leading to impairments in motor and cognitive capabilities, posing significant risks to human well-being.¹ The primary and most reliable risk factor associated with the onset of neurodegenerative conditions is increasing age, with Alzheimer's disease and Parkinson's disease being the most common.² The yearly occurrence rate of Alzheimer's disease among those aged 65 to 74 is 0.4%, rising to 3.2% in the 75 to 84

age group and further to 7.6% among those aged 85 and older.³

Acetylcholinesterase (AChE) and butyrylcholinesterase (BChE) are enzymes that play a crucial role in Alzheimer's disease (AD).⁴ AChE breaks down acetylcholine, a neurotransmitter essential for memory and learning, and inhibiting AChE can increase acetylcholine levels in the brain, potentially improving cognitive function in AD patients. BChE, which is increased in AD, further reduces acetylcholine levels.⁵ Inhibiting both enzymes can increase acetylcholine levels and improve cognitive function.⁶

Tyrosinase is an oxidoreductase involved in melanin and catecholamine

synthesis pathways.⁷ It catalyses the synthesis of dopamine for neurotransmission and catalyses the conversion from dopamine to ROS and toxic metabolites, causing oxidative stress and neurodegeneration.^{8,9,10}

Oxidative stress, an imbalance between oxidants and antioxidants, is a recognised clinical marker in AD.¹¹ It involves reactive oxygen species (ROS) and A β and is linked to elevated non-enzymatic glycation, advanced glycation end products (AGEs), and the receptor for AGEs (RAGE).^{12,13} Peroxiredoxins are an enzymatic antioxidant mechanism¹⁴ that neutralises ROS and nitrogen species. PRDX5, found in neuronal mitochondria and cytoplasm, has altered levels in various neurodegenerative diseases.¹⁵ Compounds that mimic PRDX5's antioxidant properties and biological activity are expected to treat oxidative stress-related disorders.¹⁶

Computer-aided drug design (CADD) relies on the availability of target and ligand information, using techniques like molecular mechanics, quantum mechanics, molecular dynamics, structure-based drug design, ligand-based drug design, homology modelling, ligplot analysis, molecular docking, de novo drug design, pharmacophore modelling, virtual screening, and QSARs.^{17,18}

Heterocyclic compounds, such as five-membered rings like oxadiazole and thiadiazole, interest medicinal chemists due to their unique chemical properties and diverse biological activities.^{19,20} Oxadiazoles are heterocyclic compounds with five members that contain a nitrogen atom and at least one other noncarbon ring, exhibiting a wide range of activities, including antibacterial, antimalarial, anti-inflammatory, antifungal, and anticonvulsant properties.²¹ Moreover, oxadiazoles are promising leads for developing dual-acting AChE, BuChE²², MAO-A, MAO-B²³ inhibitors for managing NDD.

Compounds with thiadiazole rings have been shown to have anticancer, anti-

inflammatory, antibacterial, antifungal, antiviral, anticonvulsant, and antiparasitic properties. Different thiadiazole hybrid structures increase their therapeutic efficacy. Thiadiazole-related compounds are identified as potential drugs to treat AD due to their ability to act as the "hydrogen binding domain," and "two-electron donor system," enabling them to create π - π stacking interactions.^{24,25}

In this study, we aim to design and synthesise eight compounds of oxadiazole/thiadiazole derivatives with heterocyclic moiety to identify novel AChE inhibitors using different *in silico* methods and to confirm their enzyme inhibitory activities.

MATERIALS AND METHODS

In silico Platform

All the *in silico* analysis was performed using Maestro 13.5.128 version of Schrodinger software 2023-1. It was programmed on a DELL 36-inch workstation, using the operating system Linux -x86_64, with Intel Core i7 processor, 1000 GB hard disk and 8GB RAM.

Molecular docking

The preparation of proteins and ligands for docking simulations involves several steps. The 3D structures of target proteins enzyme 6O4W²⁶ (acetylcholinesterase), 5I38²⁷ (tyrosinase) and 1HD2²⁸ (peroxiredoxins) were retrieved from the Protein Data Bank and refined using the Protein Preparation Wizard. Hydrogen atoms were added, bond directions were determined, and the structure was optimised using the OPLS_2005 force field. The designed thiadiazoles and oxadiazoles were prepared by ensuring they exhibited appropriate tautomeric states and underwent optimisation using the OPLS-2005 force field. The receptor grid was generated by analysing the physical characteristics within the receptor volume, and docking was performed using the Glide

module in extra precision mode²⁹. The OPLS3e force field optimised the ligand within the receptor environment, and the Glide scoring function was utilised to predict the ligands' binding affinities.

Binding free energy calculation

The MM-GBSA (Molecular Mechanics/Generalized Born Surface Area) analysis is a computational technique used to determine the binding energy of a ligand-receptor complex, measured in kcal/mol. It evaluates a ligand's propensity to bind to a receptor. It computes the binding free energy of a complex through a surface area term, a generalised Born model, and a force field derived from molecular mechanics. This method is reliable and computationally efficient for assessing the binding affinities of various ligands. A more negative value indicates stronger binding. The Schrodinger's Prime module computed the ΔG_{bind} in kcal/mol, incorporating polar and non-polar solvation models alongside molecular mechanics energies. The Prime MM-GBSA approach generates a range of energy descriptors that provide insights into the energy landscapes of ligand, receptor, and complex structures.³⁰

ADME and Physicochemical Properties

QikProp is a tool used to predict the ADME properties of drug molecules, including Caco-2 and MDCK cell permeabilities, human serum albumin binding, and HERG K⁺-channel blockage. It uses the entire 3D chemical structure for predictions, providing accurate results for molecules with unique structures. The Schrödinger QikProp module was used to assess the physicochemical attributes of ligand molecules, including octanol/water and water/gas log Ps, log S, and log BB, to determine their suitability for pharmaceutical use.^{31,32}

Chemistry

Most of the chemicals were procured from Sigma Aldrich, and melting points were determined using the capillary method

and left uncorrected. FT-IR spectral analysis, KBr discs were utilised on the Alpha Bruker FT-IR Infrared Spectrophotometer (Germany), with frequencies expressed in cm^{-1} . The Bruker Avance-II spectrometer (USA) was utilised to record ¹H-NMR spectra at 400 MHz with d₆-DMSO/CDCl₃ as a solvent, where TMS was used as an internal standard, and mass spectra were obtained using the Shimadzu LCMS 8030 (Japan), Mass spectrometer.

Synthesis and Physical Characterisation

The present study synthesises derivatives of thiadiazoles and oxadiazoles from the respective schiff base. All the reactions are carried out under standard laboratory conditions.

Synthesis of Semicarbazones and Thiosemicarbazones (3)

An equimolar mixture of semicarbazides/thiosemicarbazides (2) (0.01M) and aromatic aldehydes (1) (0.01M) was weighed and transferred into a round bottom flask, which was refluxed for 6 to 8 hours at 80°–90°C using ethanol as a solvent and catalytic amount of H₂SO₄ was added. Completion of the reaction was confirmed using TLC, and the reaction mixture was cooled, filtered and dried to separate solid particles. Finally, synthesised compounds (semicarbazones and thiosemicarbazones) are recrystallised using the solvent ethanol.³³⁻³⁶

Synthesis of Oxadiazoles and Thiadiazoles (4)

To a solution of semicarbazones/thiosemicarbazones (3) (0.001M) in 95% ethanol was slowly added an aqueous solution (6ml) of ferric chloride (649 mg, 0.004M). The reaction mixture was refluxed for 24 hours at 80°C and cooled. Solid precipitate is collected by filtration using Whatman filter paper and recrystallised from ethanol.³⁷

Spectral Data**Compound 4a: 5-(1H-indol-2-yl)-1,3,4-oxadiazol-2-amine**

Black solid; m.p.140°C; Yield: 90%; Rf: 0.75; FT-IR (cm⁻¹): 3218 (NH), 1516 (C=C), 1614 (C=N), 1455 (C-C), 1078(C-O); ¹H NMR (400 MHz, DMSO, δ/ppm): 7.02- 7.53 (m, 5H, Ar-H), 8.09 (s, 2H, NH₂), 12.17 (s, 1H, NH); Mass m/z : (M+) 201, (M+1) 202.

Compound 4d: 5-(pyridin-2-yl)-1,3,4-oxadiazol-2-amine

White solid; m.p.137°C; Yield: 65%; Rf: 0.75; FT-IR (cm⁻¹): 3399 (NH), 1746 (C=N), 1629 (C=C), 1441 (C-C), 1062 (C-O); ¹H NMR (400 MHz, DMSO, δ/ppm): 7.38 (m, 4H, Ar-H), 7.38 (s, 2H, NH₂); Mass m/z : (M⁺) 162.

Compound 4e: 5-(1H-indol-2-yl)-1,3,4-thiadiazol-2-amine

Brown solid; m.p.157°C; Yield: 91%; Rf: 0.75; FT-IR (cm⁻¹): 3288 (NH), 1457 (C=C), 1615 (C=N), 666 (C-S); ¹H NMR (400 MHz, DMSO, δ/ppm): 7.37-7.84 (m, 5H, Ar-H), 6.49 (s, 2H, NH₂), 12.03 (s, 1H, NH); Mass m/z : (M+) 217, (M+1) 218.

Compound 4g: 5-phenyl-1,3,4-thiadiazol-2-amine

Brown solid; m.p.104°C; Yield: 87%; Rf: 0.75; FT-IR (cm⁻¹): 3384.07 (NH), 1555 (C=C), 1614 (C=N), 1431 (C-C), 757 (C-S); ¹H NMR (400 MHz, DMSO, δ/ppm): 7.43-7.78 (m, 5H, Ar-H), 7.76 (s, 2H, NH₂); Mass m/z : (M+) 178, (M+1) 179.

Compound 4h: 5-(pyridin-2-yl)-1,3,4-thiadiazol-2-amine

Yellowish white solid; m.p.176 °C; Yield: 67%; Rf: 0.75; FT-IR (cm⁻¹): 3383 (NH), 1554 (C=C), 1613 (C=N), 1453 (C-C), 714 (C-S); ¹H NMR (400 MHz, DMSO, δ/ppm): 7.26-7.80 (m, 4H, Ar-H), 5.18 (s, 2H, NH₂); Mass m/z : (M+) 178.

***In vitro* Studies**

The chemicals used in the *in vitro* study were obtained from Sigma Aldrich.

Acetylcholinesterase Inhibition Assay

In this trial, 3ml of Tris. HCl buffer of pH 8.0, 20µl of substrate (0.5mM acetylcholine), 100µl of DTNB(333µM), test and standard solution in DMSO solvent (1mg/ml) which ranging from 10-50µl were taken test tubes. The mixture was allowed to incubate at 37°C for 15 minutes. Subsequently, 50 µl of AChE (5 x 10⁻¹¹ M) was introduced, and readings were recorded at 412 nm at 30-second intervals for 3 minutes. Similarly, blank and control samples were prepared, with the blank comprising buffer, substrate, and DTNB solutions.³¹

% inhibition =

$$\frac{(\text{Absorbance control} - \text{Absorbance sample})}{\text{Absorbance control}}$$

Tyrosinase Inhibition Assay

Test and standard solutions were prepared at 1 mg/ml. For testing compounds (10-50 µM) and the standard **ascorbic acid**³⁸ ref Cui HX (10-50 µM), 80 µl of 0.1 M phosphate buffer (pH 6.8) and 40 µl of L-dopa solution (1 mg/ml) were dispensed into each well of a microplate, followed by incubation at 37°C for 10 minutes. Subsequently, 40 µl of tyrosinase solution (250 U) was added to each well, and the absorbance was measured at 492 nm at intervals of 30 seconds over two minutes.³⁹

Hydrogen Peroxide Scavenging Assay

A 60 mM hydrogen peroxide solution was prepared using distilled water. The synthesised compounds and standard solutions were introduced into a hydrogen peroxide solution (0.6 ml, 40 mM) at different concentrations ranging from 50 to 250 µM. The absorbance of hydrogen peroxide at 230 nm was monitored at 30-second intervals for 2 minutes against a blank solution. Gallic acid served as the reference standard.⁴⁰

RESULTS AND DISCUSSION

Results

In silico studies

Schrodinger is the software employed for the *in silico* study of designed oxadiazole and thiadiazole analogues. Molecular docking, binding energy, ADMET properties and physicochemical parameters were evaluated.

Binding with 6O4W

Compounds **4a**, **4e**, and **4g** interacted with the acetylcholinesterase enzyme and displayed the highest docking scores of -6.62, -6.12 and -6.28 kcal/mol, respectively. Donepezil was used as a standard, which showed a docking score of -11.05 kcal/mol. The compounds **4a** and **4e** show the two hydrogen bonds with amino groups by interacting with Glu 202, Tyr 133, and Glu 202, Tyr 133. Compound **4g** has shown one hydrogen bond with the

amino acid Asn 87 via the amino group. All the **4a**, **4e**, and **4g** exhibited pi-pi stacking with substituted benzene and heterocycles via amino acid Tyr 337. The standard donepezil interacted with the protein with the amino acids Trp 286 and Trp 86, undergoing pi-pi stacking and hydrogen bonding with Phe 295. Compared to standard, **4a**, **4e** and **4g** show common hydrophobic interactions with amino acid residues Tyr 337 and Phe 338. **4a**, **4e** and donepezil also show hydrophobic interaction with residues, Tyr 133, Ile 451. The residue His 447 is involved in polar interaction with compounds **4a**, **4e**, **4g** and standard (**Fig. 1-3**, **Table 1-2**). The residue His 447 plays a crucial role in polar interactions with certain compounds. For instance, in acetylcholinesterase (AChE), His 447 interacts with the standard donepezil. These compounds exhibit strong binding energies and form hydrogen bonds with His 447.⁴¹

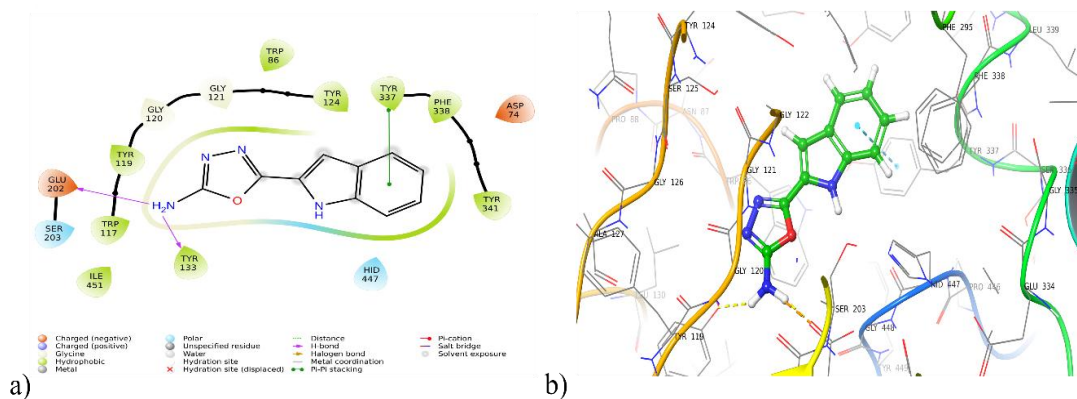


Fig. 1: Represents a) 2D and b) 3D interaction of compounds **4a** with 6O4W.

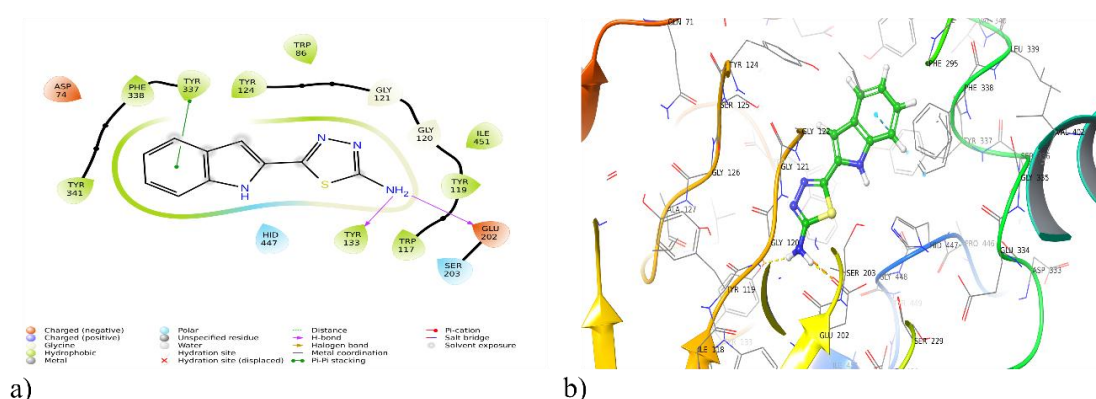


Fig. 2: Represents a) 2D and b) 3D interaction of compounds **4e** with 6O4W.

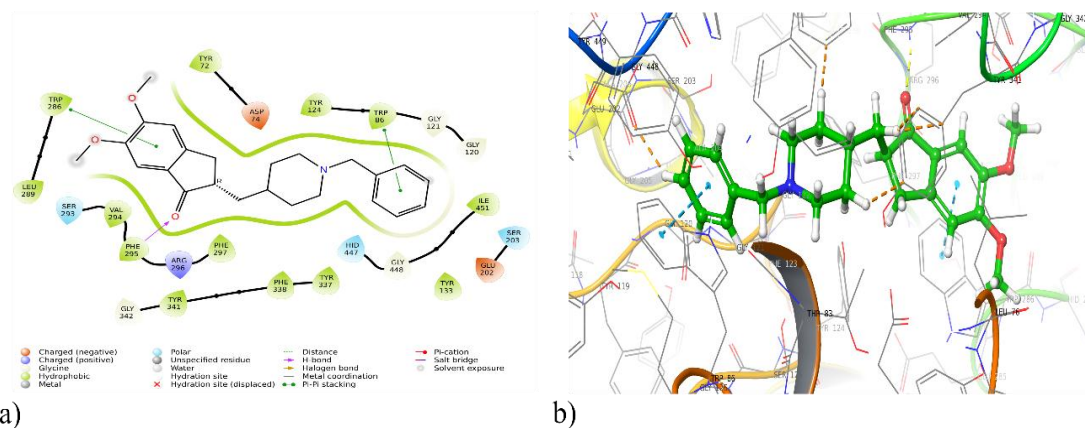


Fig. 3: Represents a) 2D and b) 3D interaction of donepezil with 6O4W.

Table 1: Docking score of oxadiazole and thioadiazole analogues with the target proteins 6O4W, 5I38 and 1HD2.

SI NO.	Compounds	Proteins	G score
1	4a	6O4W	-6.622
		5I38	-5.115
		1HD2	-2.008
2	4b	6O4W	-4.901
		5I38	-3.952
		1HD2	-2.142
3	4c	6O4W	-5.754
		5I38	-3.746
		1HD2	-2.143
4	4d	6O4W	-5.860
		5I38	-2.967
		1HD2	-1.957
5	4e	6O4W	-6.286
		5I38	-5.264
		1HD2	-1.878
6	4f	6O4W	-5.051
		5I38	-3.268
		1HD2	-2.040
7	4g	6O4W	-6.126
		5I38	-3.700
		1HD2	-1.621
8	4h	6O4W	-5.166
		5I38	-3.472
		1HD2	-1.833
9	Co-crystals	6O4W	-11.105
		5I38	-5.424
		1HD2	-5.506

*Co-crystals - 6O4W (Donepezil); 5I38 (Kojic acid); 1HD2 (Gallic acid).

Table 2: Docking interaction of designed oxadiazole and thiadiazole compounds with target proteins 6O4W, 5I38 and 1HD2.

SI NO.	Compounds	Proteins	Hydrogen bond	Polar interaction	Hydrophobic interaction	Pi-Pi stacking
1	4a	6O4W	Glu 202, Tye 133	Ser 304, Hid 447	Trp 117, Tyr124, Tyr 337, Tyr 133, Tyr 341, Phe 338, Ile 451	Tyr 337
		5I38	His 204, Glu 195	His 60, His 204, Asn 205, His 208	Ala 221, Val 218, Val 217, Met 215, Phe 197, Met 61, Phe 65	His 60
		1HD2	Thr 147	Thr 44, Thr 147	Phe 120, Pro 40, Pro 45, Cys 47, Leu 149	-
2	4b	6O4W	Ser 293, Tyr 341	Ser 293	Phe 297, Tyr 124, Phe 295, Val 294, Tyr 341, Trp 286, Phe 338, Tyr 337	Trp 286
		5I38	Glu 195, His 204	His 60, His 204, Asn 205, His 208	Met 215, Val 217, Val 218, Ala 221, Phe 197, Met 61, Phe 65	His 60
		1HD2	Thr 147	Thr 44, Thr 147	Pro 120, Ile 119, Pro 45, Leu 116, Leu 149	-
3	4c	6O4W	Asn 87	His 447, Asn 87, Thr 83, Ser 125	Tyr 337, Phe 338, Tyr 341, Trp 86, Tyr 124	Phe 338
		5I38		His 231, His 42, His 60, His 208, Asn 205, His 204	Met 215, Val 217, Val 218, Ala 221, Phe 227, Pro 222, Phe 65	His 208
		1HD2	Thr 147	Thr 44	Leu 116, Ile 119, Phe 120, Pro 45, Cys 47, Pro 40	Phe 120
4	4d	6O4W	Tyr 124	Ser 125	Phe 297, Trp 286, Tyr 124, Trp 86, Tyr 337, Phe 338, Tyr 341	Tyr 337
		5I38	-	His 42, His 60, His 69, His 231, His 208, His 204, Asn 205	Met 215, Val 217, Val 218, Phe 227, Ala 221, Phe 65	His 60, His 208
		1HD2	-	Thr 44, Thr 147	Leu 116, Ile 119, Phe 120, Pro 45, Pro 40	Phe 120

Table 2: Continued.

5	4e	6O4W	Glu 202, Tyr 133	Ser 203, His 447	Ile 451, Trp 117, Tyr 133, Tyr 119, Trp 86, Tyr 124, Tyr 337, Phe 338, Tyr 341	Tyr 337
		5I38	Asn 205	His 60, His 208, His 204, Asn 205, Hie 42, His 231	Met 215, Val 217, Val 218, Ala 221, Pro 222, Phe 227, Pro 201, Phe 65	His 60, His 208
		1HD2	Thr 147	Thr 44, The 147	Pro 45, Leu 149, Pro 40, Phe 120, Ile 119	-
6	4f	6O4W	Asn 87	Thr 83, Asn 87, Ser 125, Hid 447	Trp 86, Tyr 124, Tyr 337, Phe 338, Tyr 341	Tyr 337
		5I38	His 60	His 204, Asn 205, His 208, His 231, Hie 42, His 69, His 60,	Ala 221, Val 218, Phe 197, Met 61, Phe 227	His 208, His 60
		1HD2	Thr 147	Thr 44, The 147	Pro 45, Leu 149, Ile 119, Phe 120	-
7	4g	6O4W	Asn 87	Hid 447, Asn 87, Ser 125	Tyr 341, Phe 338, Tyr 337, Tyr 124, Trp 86	Tyr 337
		5I38	-	His 208, Asn 205, His 204, Hie 42, His 231, His 60	Met 215, Val 217, Val 218, Phe 227, Ala 221, Pro 201, Phe 197	His 208
		1HD2	Gly 46	Thr 44, The 147	Pro 45, Cys 47, Leu 149, Leu 116, Pro 40, Phe 120	-
8	4h	6O4W	Phe 295	Ser 293	Tyr 124, Trp 286, Val 294, Phe 295, Phe 297, Tyr 341, Phe 338, Tyr 337	Tyr 341
		5I38	His 60	His 231, His 69, His 208, Hie 42, Asn 205, His 60, His 204	Val 218, Ala 221, Phe 227, Met 61, Pro 201, Phe 197	His 208, His 204, His 60
		1HD2	-	Thr 44, The 147	Pro 40, Leu 116, Ile 119, Phe 120	-

Table 2: Continued.

9	Co-crystals	6O4W	Phe 295	Ser 293, His 447, Ser 203	Trp 286, Leu 289, Tyr 72, Tyr 124, Tyr 86, Val 294, Phe 295, Phe 297, Tyr 341, Phe 338, Tyr 337, Tyr 133, Ile 451	Trp 86, Trp 286
		5I38	His 42, Gly 216	His 204, Asn 204, His 208, His 60, His 42, His 231	Met 215, Val 217, Val 218, Phe 65, Ala 221, Phe 227	His 208
		1HD2	Gly 46, Cys 47, Thr 44, Arg 127	Thr 44, Thr 147	Leu 116, Ile 119, Phe 120, Leu 112, Pro 40, Pro 45, Cys 47	Phe 120

*Co-crystals - 6O4W (Donepezil); 5I38 (Kojic acid); 1HD2 (Gallic acid).

Binding with 5I38

4e, 4a and 4b have exhibited better docking scores of -5.26, -5.11 and -3.95 kcal/mol, when they interacted with the enzyme tyrosinase. Compounds 4e and 4a have exhibited one hydrogen bonding with the amino acid Asn 205 via “NH” of substituted indole, and they both have interacted with the amino acids His 60 and His 208 via benzene ring of substituted indole resulting in a substantial pi-pi stacking. In contrast, compound 4b has shown a pi-pi stacking alone with the amino acid His 60 via oxadiazole moiety. The standard kojic acid showed a docking

score of -5.42 kcal/mol, where it showed two hydrogen bonds with amino acids Gly 216 and His 60 via hydroxyl group and pi-pi stacking with His 208 in the aromatic ring. Compared to standard kojic acid, hydrophobic interactions with amino acids Met 215, Val 217, Val 218, Ala 221 and polar interaction with amino acid residues His 60, His 208, and His 204 are common in compounds 4e, 4a, 4b (**Fig. 4-6, Table 1-2**).

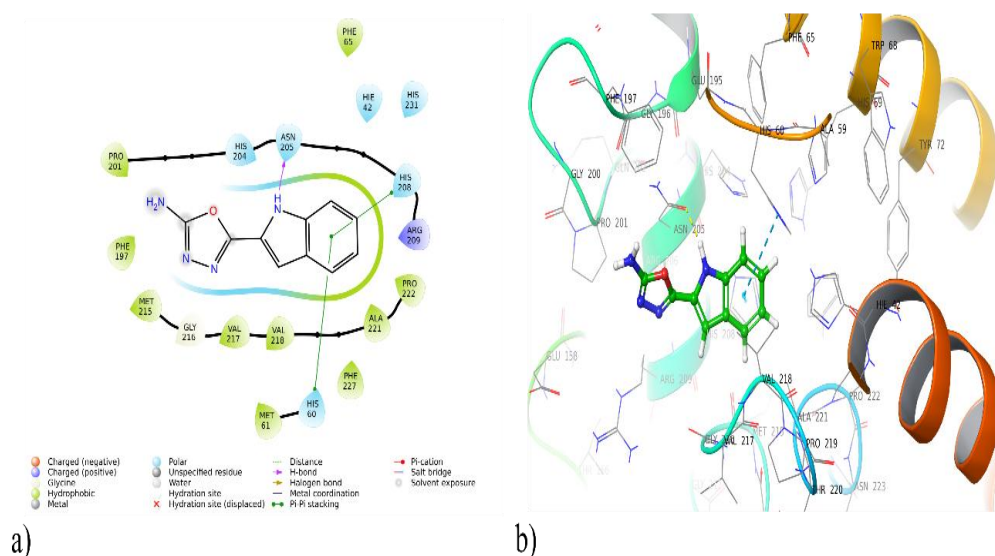


Fig. 4: Represents a) 2D and b) 3D interaction of compounds 4a with 5I38.

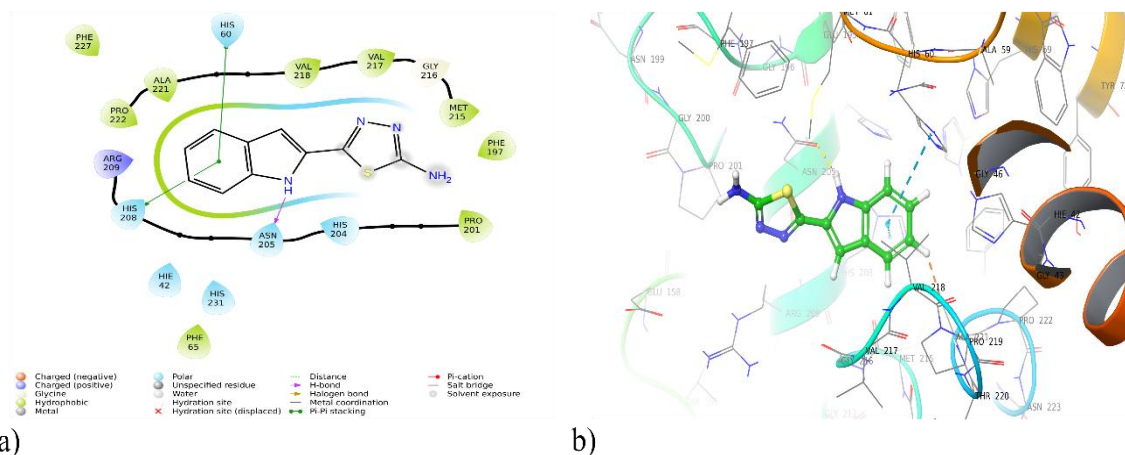


Fig. 5: Represents a) 2D and b) 3D interaction of compounds 4e with 5I38.

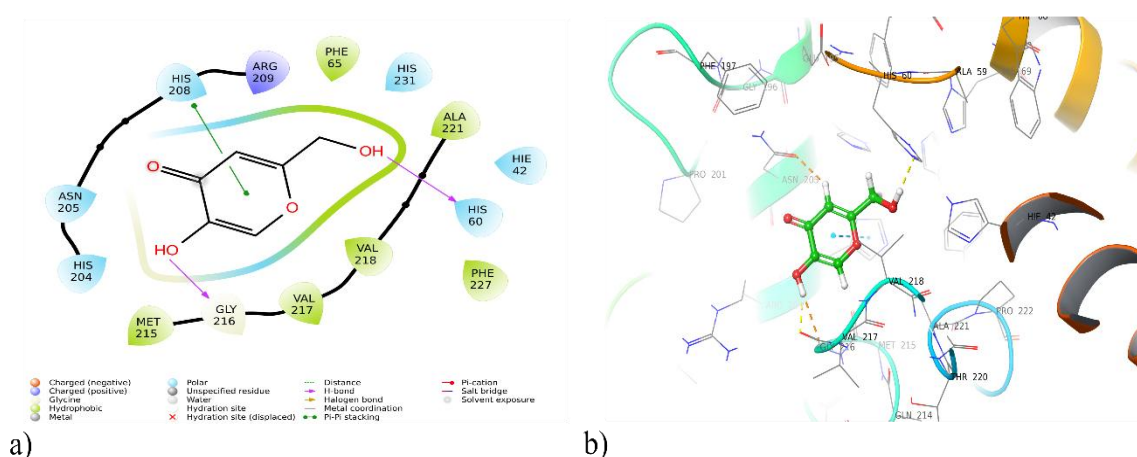


Fig. 6: Represents a) 2D and b) 3D interaction of kojic acid with 5I38.

Binding with 1HD2

Compounds 4b and 4c exhibited an enhanced interaction within the pockets of protein 1HD2 with amino acid Thr 147 undergoing hydrogen bonding via the amino group by showing a docking score of -2.14 kcal/mol, followed by 4f and 4a with a docking score of -2.04 and -2.00 kcal/mol. Whereas the standard shows a docking score of -5.50 kcal/mol, with the four hydrogen bonding taking place in the amino acids Cys 47, Gly 46, Thr 44 and Arg 127 via carboxylic acid group and pi-pi stacking with amino acids Phe 120 via aromatic ring in gallic acid. Apart from this, compounds 4b and 4c exhibit the common hydrophobic interaction with amino acid residues Ile 119, Pro 45, and Leu 116 and polar

interaction with Thr 147, also found in the standard (**Fig. 7-9, Table 1-2**).

By evaluating the *in silico* inhibitory binding interactions concerning amino acids of the compounds with various targets like acetylcholine esterase (Phe 338, Tyr 341, and Tyr 337), tyrosinase (His 204, His 60, Asn 205, His 208, His 208, Ala 221, Val 218 and His 60) and peroxiredoxin (Thr 147, Thr 44, Phe 120) it was found that the compounds share common interactions with amino acid residues of active sites. This indicates that all the ligands are binding to the same active site; hence, we can conclude that it's a competitive type of binding inhibition.

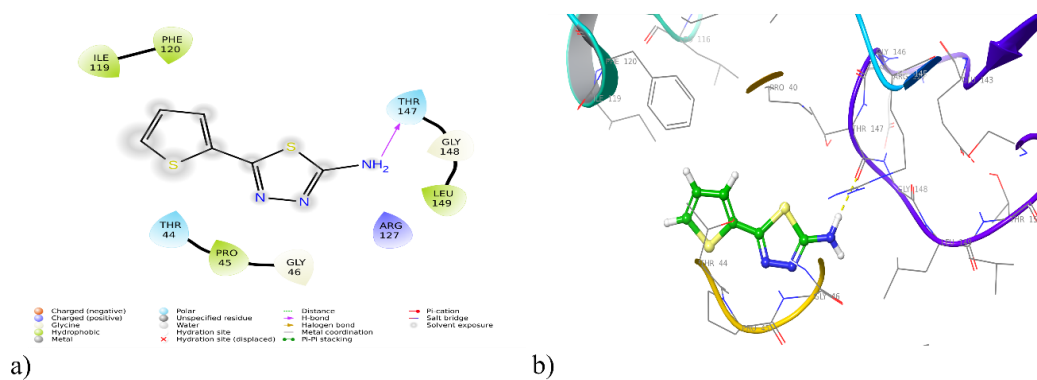


Fig. 7: Represents a) 2D and b) 3D interaction of compounds 4b with 1HD2.

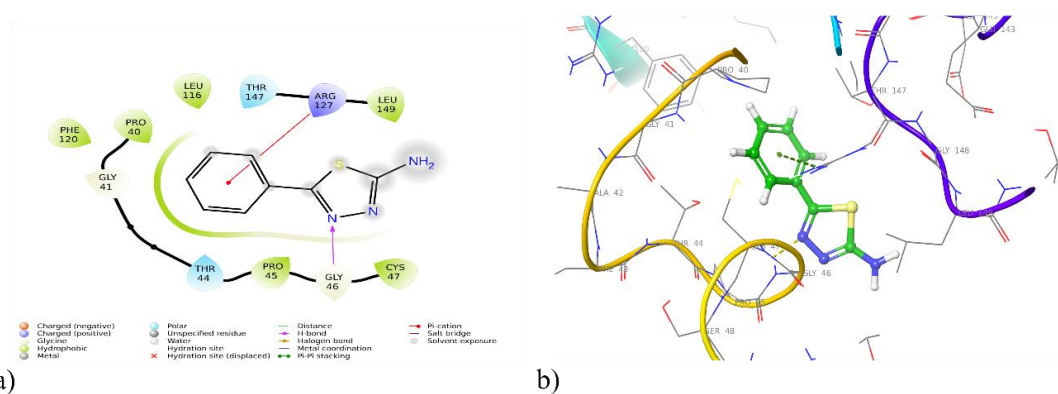


Fig. 8: Represents a) 2D and b) 3D interaction of compounds 4c with 1HD2.

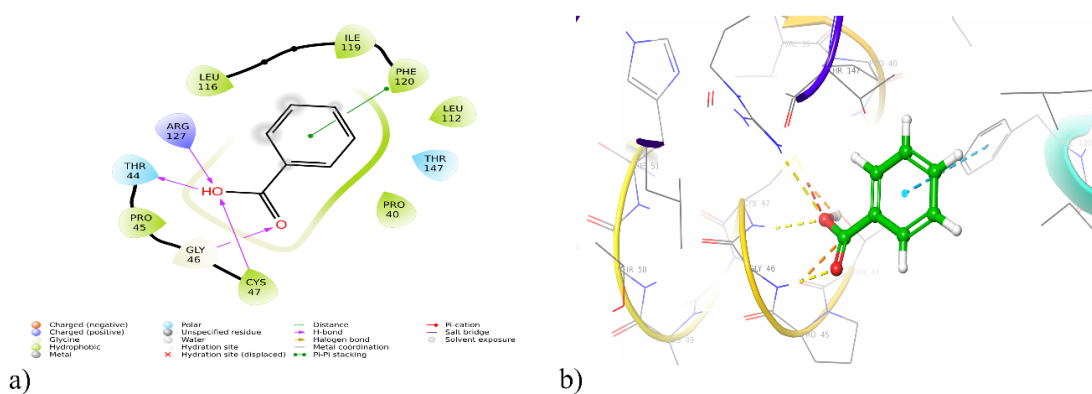


Fig. 9: Represents a) 2D and b) 3D interaction of benzoic acid with 1HD2.

Binding Free Energy Calculations

The binding free energy of ligand-protein complexes was predicted by the MM-GBSA method, validating docking results. The ΔG bind values ranged from -16.04 to -43.60 kcal/mol for 6O4W and -27.52 to -42.70 kcal/mol for 5I38. Non-

polar solvation and van der Waals energies were the main contributors to the interaction. The best-interacted compound 4a showed a binding free energy of -28.23 kcal/mol, and the co-crystal of peroxiredoxin had a binding free energy of -40.26 kcal/mol (**Table 3**).

Table 3: Binding free energy calculation of designed oxadiazole and thiadiazole compounds with target proteins 6O4W, 5I38 and 1HD2.

SI NO.	Compounds	Proteins	ΔG bind (Kcal/mol)	ΔG bind Coulomb	ΔG bind covalent	ΔG bind H Bond	ΔG bind Lipophilic	ΔG bind Solv GB	ΔG bind Vander
1	4a	6O4W	-25.39	-7.54	0.00	-3.02	-15.81	34.49	-30.58
		5I38	-37.42	-14.20	3.33	-0.25	-16.66	28.14	-31.80
		1HD2	-28.23	-9.76	2.01	-0.24	-12.88	10.68	-18.05
2	4b	6O4W	-38.95	-13.30	0.00	-1.76	-18.77	19.48	-23.19
		5I38	-39.68	-14.75	1.24	-2.97	-15.69	17.16	-23.79
		1HD2	-30.09	-14.11	1.15	-1.22	-12.71	11.81	-14.70
3	4c	6O4W	-16.04	-3.14	0.00	-0.80	-11.45	24.51	-23.82
		5I38	-32.73	-2.68	0.93	-0.17	-14.03	16.85	-27.21
		1HD2	-22.77	-2.50	0.18	-0.75	-10.23	2.72	-12.00
4	4d	6O4W	-24.78	-8.94	0.00	-1.01	-11.08	19.32	-22.03
		5I38	-31.42	-10.00	4.60	-1.39	-11.39	18.25	-27.44
		1HD2	-23.46	-14.15	0.30	-0.75	-8.26	14.25	-13.39
5	4e	6O4W	-31.69	-9.77	0.00	-2.95	-22.73	40.64	-33.14
		5I38	-42.70	-17.42	3.75	-0.24	-20.33	31.83	-33.64
		1HD2	-32.75	-9.58	1.33	-0.93	-16.57	10.57	-17.57
6	4f	6O4W	-23.03	-0.65	0.00	-0.76	-19.04	29.06	-28.57
		5I38	-32.57	-1.20	3.06	-0.70	-19.58	21.40	-31.79
		1HD2	-32.34	-12.91	0.59	-1.04	-15.60	11.84	-15.23
7	4g	6O4W	-21.42	-1.95	0.00	-0.80	-17.25	30.41	-29.07
		5I38	-35.51	-8.23	2.64	-0.00	-17.02	23.69	-32.24
		1HD2	-32.12	-8.26	2.29	-0.22	-16.66	12.53	-20.62
8	4h	6O4W	-43.60	-12.33	0.00	-0.63	-17.98	20.59	-27.77
		5I38	-29.62	-0.26	3.70	-0.69	-14.67	16.35	-30.52
		1HD2	-26.11	-6.66	0.38	-0.73	-12.52	8.47	-14.09
9	Co-crystals	6O4W	-73.90	-13.63	0.00	-0.25	-51.27	55.14	-54.95
		5I38	-40.26	-21.02	1.11	-0.52	-11.96	18.10	-23.17
		1HD2	-27.37	-17.74	2.34	-1.23	-9.96	10.53	-10.50

*Co-crystals - 6O4W (Donepezil); 5I38 (Kojic acid); 1HD2 (Gallic acid).

ADMET Physicochemical Properties

The pharmacokinetic and physicochemical properties of the compounds were determined using QikProp, which helps in understanding the absorption, distribution, metabolism, and elimination of the compounds, as well as their onset of action and penetration through the blood-brain barrier. The tool assessed bioavailability, blood-brain barrier

penetration, plasma-protein binding, metabolism, HERG K, and solvent-accessible surface area to aid medicinal chemists in improving the compounds' activity. Physicochemical properties will help to identify the drug-likeness properties of the compounds. Varied physicochemical properties of synthesised 1,3,4-oxadiazol-2-amine and 1,3,4-thiadiazol-2-amine derivatives were measured (Table 4 and 5).

Table 4: ADMET properties of designed oxadiazole and thiadiazole compounds.

SI NO.	Compounds	%HOA	#metab	QPlog S	QPlog HERG	QPlog Caco	QPlog BB	CNS	QPlog Khsa	QPlog MDCK
Acceptable range		>80% High <25% Low	(1-8)	-6.5 to -0.5	Below -5	>500 Great <25 Poor	-3.0 to 1.2	-2 to +2	-1.5 to 1.5	>500 Great <25 Poor
1	4a	78.42	1	-2.22	-4.49	365.29	-0.76	-1	-0.35	166.58
2	4b	82.49	2	-1.61	-3.58	545.44	-0.42	-1	-0.53	462.31
3	4c	83.14	1	-1.68	-4.09	580.20	-0.54	-1	-0.46	274.66
4	4d	74.70	2	-1.39	-3.83	400.61	-0.66	-1	-0.59	184.05
5	4e	84.41	1	-2.84	-4.67	488.35	-0.58	-1	-0.22	395.80
6	4f	87.08	2	-2.24	-3.83	647.86	-0.29	0	-0.40	961.52
7	4g	87.69	1	-2.21	-4.14	701.48	-0.38	0	-0.33	565.81
8	4h	80.80	2	-1.97	-4.01	545.84	-0.47	-1	-0.47	443.54
9	Donepezil	100.00	6	-4.57	-6.67	874.38	0.10	1	0.58	473.38
10	Kojic acid	66.12	2	-2.76	-3.20	247.09	-0.93	-1	-0.86	109.17
11	Gallic acid	80.64	0	-1.483	-1.72	244.81	-0.30	-1	-0.67	137.46

%HOA- %Human Oral Absorption, **#metab**- Number of likely metabolic reactions, **QPlogS**- Aqueous solubility, **QPlogHERG**- IC₅₀ value for blockage of HERG K⁺ channels, **QPlog Caco**-Apparent Caco-2 cell permeability, **QPlogBB**- Brain/Blood partition coefficient, **CNS**- Central Nervous System activity, **QPlog Khsa**- Binding to human serum albumin, **QPlog MDCK**- apparent Madin-Darby canine kidney (MDCK) cell permeability.

Table 5: Physicochemical properties of designed oxadiazole and thiadiazole compounds.

SI NO.	Compounds	Mol.Wt	DonorHB	Accept HB	QPlog _{o/w}	PSA	RO5	RO3
Acceptable range		≤500	≤5	≤10	(-2.0 to 6.5)	7– 200	< 4	< 3
1	4a	200.19	3	3	0.95	79.50	0	0
2	4b	167.18	2	3	1.12	66.61	0	0
3	4c	161.16	2	3	1.15	65.49	0	0
4	4d	162.15	2	4	0.20	77.04	0	0
5	4e	216.26	3	3	1.59	68.36	0	0
6	4f	183.24	2	3	1.67	56.29	0	0
7	4g	177.22	2	3	1.67	55.73	0	0
8	4h	178.21	2	4	0.83	65.80	0	0
9	Donepezil	379.49	0	5	4.35	49.77	0	0
10	Kojic acid	142.11	2	5	-0.62	81.27	0	0
11	Gallic acid	122.12	1	2	1.86	50.37	0	0

Mol.Wt- Molecular Weight, **Donor HB**- Hydrogen Bond Donor, **Accept HB**- Hydrogen Bond Acceptor, **QPlog_{o/w}**- Predicted octanol/water partition coefficient, **PSA**- Polar Surface Area, **RO5**- Rule of Five, **RO3**- Rule of Three.

Bioavailability Prediction

The assessment of oral absorption includes measures such as expected aqueous solubility (logS), predicted % human oral absorption, and adherence to Jorgensen's "Rule of Three (RO3)." Meeting criteria like logS > -5.7, Caco-2 > 22 nm/s, and having fewer than 7 primary metabolites indicates oral accessibility. The compounds tested showed high permeability across the gut-blood barrier

and compliance with Jorgensen's RO3, indicating their oral bioavailability (**Table 4**).

Prediction of Blood-Brain Barrier (BBB) Penetration

Qlog BB predicts the brain/blood coefficient for orally delivered drugs, indicating their ability to cross the blood-brain barrier and reach the central nervous system (CNS). In the study, all synthesised

compounds had Qlog BB values within the acceptable range of -3.0 to 1.2. Compounds 4a, 4d, and 4e showed expected values of -2 to 2, suggesting higher activity in the CNS. Compounds 4f and 4g also exhibited greater QPlogMDCK values (>500), indicating their potential efficacy and activity in the CNS (**Table 4**).

Prediction of Plasma-Protein Binding

The binding of the drugs to plasma proteins decreases the number of medications reaching the blood circulation, affecting drug efficiency. The plasma protein binding is determined by binding to human serum albumin (log KHSA) (recommended range is -1.5 to 1.5). The derivatives are likely to reach the blood circulation freely, thus making them more available to the target site (**Table 4**).

Metabolism Prediction

All the synthesised compounds are predicted to undergo metabolism below eight; hence, the metabolic rates are within the recommended number (**Table 4**).

Prediction of Blockage of Human Ether-A-Go-Go-Related Gene Potassium (HERG K⁺) Channel

HERG K⁺ channel blockers are potentially toxic, and the predicted IC₅₀ values often provide reasonable predictions for the cardiac toxicity of drugs in the early stages. Standard donepezil shows an IC₅₀ less than -5, and the rest of the synthesised compounds show an IC₅₀ value in the permissible limit (**Table 4**).

Prediction of Solvent-Accessible Surface Area (SASA, FOSA, FISA, PISA, WPSA)

The solvent-accessible surface area (SASA) measurements for the synthesised compounds were within standard limits, typically ranging from 300 to 1000 Å. The hydrophobic component (FOSA) and hydrophilic component (FISA) of SASA,

along with the π -component (PISA) and weakly polar component (WPSA), were all within acceptable ranges. FOSA values were within 0-750, FISA values ranged from 7.0 to 330.0, PISA values were normal (0.0-450.0), and WPSA values fell within 0.0-175.0. These results indicate that all drug candidates met the criteria for these surface area parameters, suggesting their suitability for further evaluation and development (**Table 4**).

Chemistry

The synthesis involved two-step reactions; the first step involved the synthesis of the schiff base. The reactions occur between substituted aldehydes, a nucleophilic addition reaction with the elimination of water to form semicarbazone and thiosemicarbazone, respectively. The second step involved the cyclisation of Schiff-based intermediate in the presence of ferric chloride to yield substituted 1,3,4-oxadiazol-2-amine and 1,3,4-thiadiazol-2-amine, respectively. Synthesis of oxadiazoles (4a and 4d) and thiadiazoles (4e, 4g and 4h) was possible and resulted in good yield by the above reaction (**Fig. 10**). The final structure of synthesised derivatives is confirmed by using IR spectra, where the peaks between 1000-1250 cm⁻¹ correspond to C-O-C stretch, as in compound 4a, where it showed at 1098.27 cm⁻¹ and 1,3,4-thiadiazol-2-amine shows the peak in the range 600-800 cm⁻¹ of C-S-C stretch, which corresponds to 744.21 cm⁻¹ in compound 4e, showing that the cyclisation has taken place. In compound 4a, the ¹H NMR spectra show a peak corresponding to the aromatic ring at 7.02-7.53 ppm (m, 5H), an amine peak at 8.09 ppm (d, 2H) and an NH group in the indole, which corresponds to 12.17 ppm (s, 1H). Mass spectra of compound 4a show M⁺ and M⁺¹ peaks at 201 and 202 m/z.

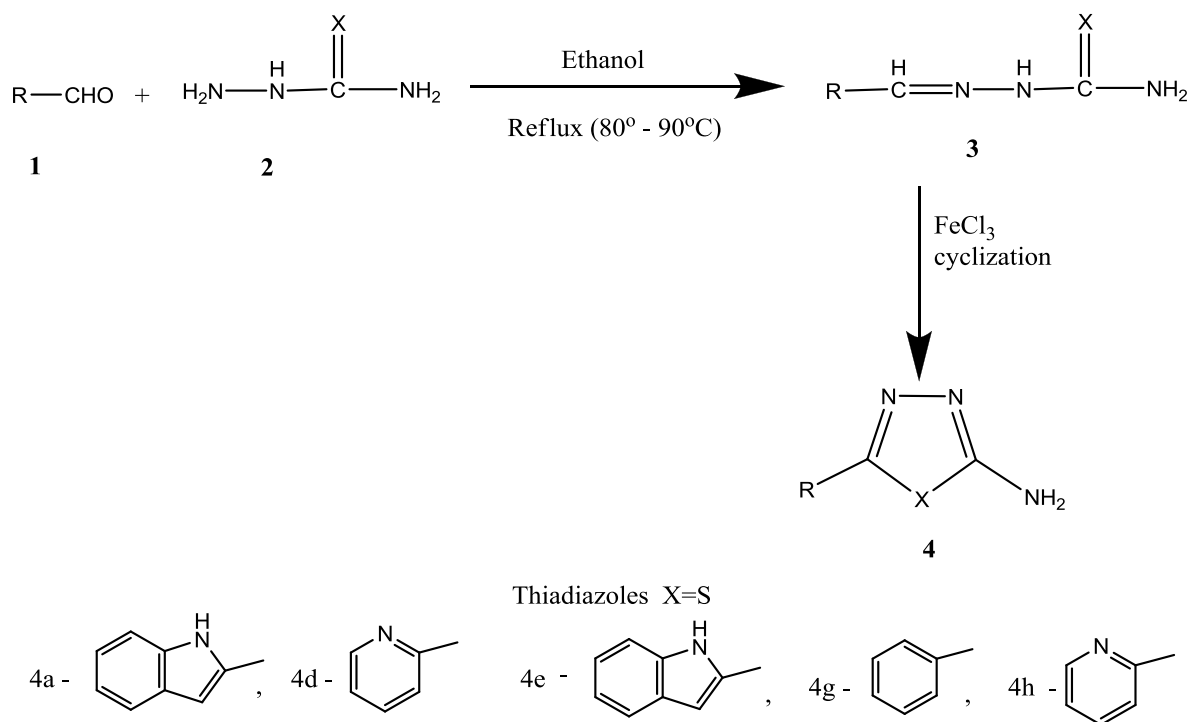


Fig. 10: Scheme of synthesis.

In vitro studies

Acetylcholinesterase Enzyme Inhibition Assay

Synthesised oxadiazoles (4a and 4d) and thiadiazoles (4e, 4g and 4h) were subjected to determine the inhibitory potency against human AChE using Ellman's method. Where all the compounds were active and have shown IC_{50} values below $100\mu\text{M}$. Compound 4a exhibited the

highest inhibitory activity with an IC_{50} value of 3.73 ± 0.01 , corresponding with docking data showing good docking results of -6.63 with the interacted protein. This is followed by compound 4e (IC_{50} is $8.73 \pm 1.00 \mu\text{M}$), with a good docking score of -6.28 kcal/mol respectively. The standard donepezil exhibited an IC_{50} value of $4.38 \pm 0.53 \mu\text{M}$ (**Table 6**).

Table 6: Data of acetylcholine esterase inhibitory activity of oxadiazole and thiadiazole derivatives by Ellman's method.

Sample code	Percentage inhibition					IC_{50}	Docking Scores
	$10\mu\text{M}$	$20\mu\text{M}$	$30\mu\text{M}$	$40\mu\text{M}$	$50\mu\text{M}$		
4a	17.05	35.49	45.08	61.14	55.31	3.73 ± 0.01	-6.622
4d	85.93	87.50	87.42	87.03	93.15	23.07 ± 0.73	-5.860
4e	67.40	73.90	70.00	72.00	80.02	8.73 ± 1.00	-6.286
4g	84.24	85.40	83.50	85.75	82.00	87.70 ± 0.77	-6.126
4h	74.96	74.76	76.50	78.04	77.40	28.50 ± 0.52	-5.166
Donepezil	57	65	75	85	93.4	4.38 ± 0.53	-11.105

Tyrosinase Inhibitory Effect

All the compounds were active with good IC_{50} values below 50 μM . Compound 4e has shown good inhibitory activity of IC_{50} values of $1.36 \pm 0.06 \mu M$, which complies with the docking results where they exhibit excellent docking scores of -5.26 kcal/mol. This was followed by compound 4a with the IC_{50} value of $2.59 \pm 0.06 \mu M$, whereas ascorbic acid was used as standard, showing the IC_{50} value of $1.71 \pm 0.10 \mu M$ (Table 7).

Hydrogen Peroxide Scavenging Assay

The hydrogen peroxide scavenging assay was performed to confirm if the synthesised compound has antioxidant activity. The ability of a compound to

scavenge peroxides was compared to that of standard gallic acid. The study was based on the idea that antioxidants catalyse the conversion of hydrogen peroxide into water and oxygen. The compounds 4d ($IC_{50} = 7.35 \pm 0.22 \mu M$) and 4a ($IC_{50} = 9.26 \pm 0.19 \mu M$) reported the highest scavenging activity, and the results aligned with *in silico* studies. Standard gallic acid has an IC_{50} value of $4.32 \pm 0.39 \mu M$ (Table 8).

By correlating all the *in vitro* studies for the most active compound, 4a, for comparisons with respect to three targets, we confirm that the type of enzyme inhibition is a competitive type of binding inhibition, as all the concentrations pass through the origin (Fig. 11).

Table 7: Data of tyrosinase inhibitory activity of oxadiazole and thiadiazole derivatives.

Sample code	Percentage inhibition (%)					IC_{50}
	10 μM	20 μM	30 μM	40 μM	50 μM	
4a	39.50	33.50	42.25	71.54	84.20	2.59 ± 0.06
4d	24.76	34.76	48.09	51.49	56.49	3.64 ± 0.13
4e	47.50	50.25	70.25	77.25	91.25	1.36 ± 0.06
4g	86.50	85.25	89.25	90.25	93.62	19.05 ± 0.98
4h	19.50	28.50	42.98	67.24	72.07	3.26 ± 0.02
Ascorbic acid	65.23	61.2	78.5	74.7	83.55	1.71 ± 0.10

Table 8: Data of hydrogen peroxide scavenging activity of oxadiazole and thiadiazole derivatives.

Sample code	Percentage inhibition					IC_{50}
	10 μM	20 μM	30 μM	40 μM	50 μM	
4a	57.14	65.43	69.12	75.11	80.18	9.26 ± 0.19
4d	35.48	49.76	51.15	63.13	64.97	7.35 ± 0.22
4e	80.18	82.94	85.25	92.62	90.50	17.48 ± 0.56
4g	61.29	63.13	63.59	72.35	75.57	14.71 ± 0.78
4h	65.43	73.73	78.43	82.94	83.87	11.04 ± 0.36
Gallic acid	9.8	20	37	48.9	64	4.32 ± 0.39

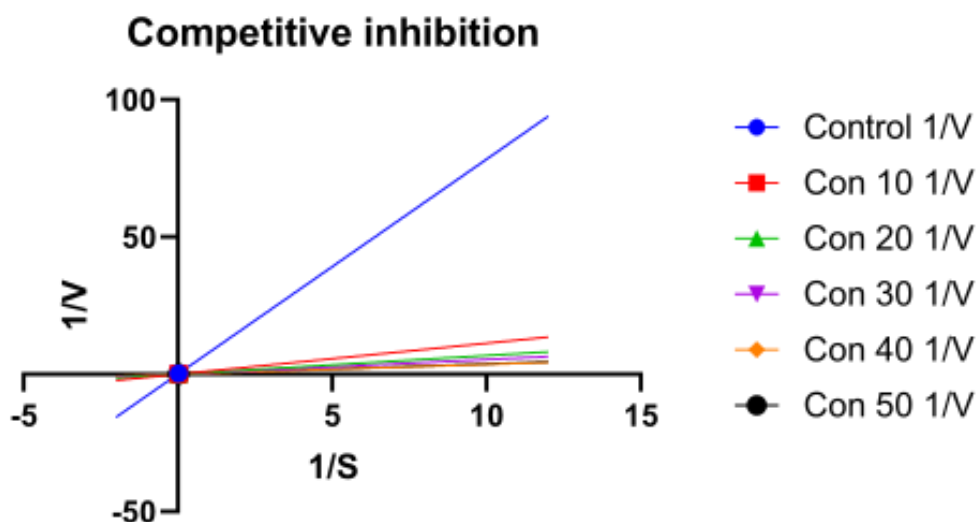


Fig. 11: Inhibitory kinetics of compound 4a.

Structural activity relationship

By correlating the docking and biological activity studies, 5-(1H-indol-2-yl)-1,3,4-oxadiazol-2-amine (4a) is the oxadiazole series's most potent AChE and tyrosinase inhibitor. The synthesised compound comprised a five-membered oxadiazole linked with an indole moiety. On the other hand, 5-(1H-indol-2-yl)-1,3,4-thiadiazol-2-amine (4e) is the most active compound against the acetylcholinesterase and tyrosinase enzymes, among the series of thiadiazoles.⁴² On further analysis of both moieties (oxadiazoles and thiadiazoles) biological action, compounds with indole heterocyclic groups, i.e., 4a and 4e, are found to be active as acetylcholinesterase and tyrosinase inhibitors, followed by thiophene heterocyclic groups,⁴³ as in the cases of 4b and 4f. These led to the analysis of the result in the absence of heterocyclic groups, for example, compounds 4c and 4g, where only the benzaldehyde group is present, and it was found that inhibitory action was less. Therefore, from the above observations, we can infer that the presence of heterocyclic groups might increase the biological action compared to compounds without heterocyclic groups.⁴⁴ Thus, this study indicates that an indole-based oxadiazole/thiadiazole can be a promising

candidate for developing a preferred drug for NDD, as these compounds have demonstrated the highest levels of inhibition against acetylcholinesterase and tyrosinase enzymes, along with remarkable effectiveness in scavenging peroxide.

Conclusion

A novel series of substituted 1,3,4-oxadiazol-2-amine (4a-4d) and 1,3,4-thiadiazol-2-amine (4e-4h) derivatives were designed and subjected to *in silico* studies. By comparing the docking results and biological data of synthesised derivatives, it has been found that the compounds 5-(1H-indol-2-yl)-1,3,4-oxadiazol-2-amine (4a) and 5-(1H-indol-2-yl)-1,3,4-thiadiazol-2-amine (4e) is showing most potent activity against the enzyme acetylcholinesterase, tyrosinase and peroxiredoxins, which attributes to their neuroprotective action. Based on the docking scores and synthesis feasibility, oxadiazole (4a, 4d) and thiadiazole (4e, 4g, 4h) derivatives were synthesised from the intermediate Schiff Bases and characterised by spectral data. These compounds were further evaluated by biological studies. The *in vitro* results analysis found that compounds 4a and 4e exhibited the highest inhibitory activity against the enzyme acetylcholinesterase and were also good antioxidant agents.

REFERENCES

1. A.D. Gitler, P. Dhillon and J. Shorter, "Neurodegenerative disease: models, mechanisms, and a new hope," *Dis Model Mech*, 10(5),499-502 (2017).
2. C.M. Tanner, "Epidemiology of Parkinson's disease", *Neurol Clin*, 10, 317- 329 (1992).
3. L.L. Raket, "Statistical disease progression modeling in Alzheimer disease", *Front Big Data*, 3, 24 (2020).
4. J. H. Heo, B.H. Eom, H.W. Ryu, M.G. Kang, J.E. Park, D.Y. Kim, J.H. Kim, D. Park, S.R. Oh, and H. Kim, "Acetylcholinesterase and butyrylcholinesterase inhibitory activities of khellactone coumarin derivatives isolated from *Peucedanum japonicum* Thurnberg", *Sci Rep*, 10(1), 21695 (2020).
5. X.Q. Chen and W.C. Mobley, "Exploring the pathogenesis of Alzheimer disease in basal forebrain cholinergic neurons: converging insights from alternative hypotheses", *Front Neurol*, 13, 451499 (2019).
6. M.S. García-Ayllón, D. H. Small, J. Avila and J. Sáez-Valero, "Revisiting the role of acetylcholinesterase in Alzheimer's disease: cross-talk with P-tau and β -amyloid", *Front Mol Neurosci*, 4,22 (2011).
7. D. Sulzer, J. Bogulavsky, K. E. Larsen, G. Behr, E. Karatekin, M. H. Kleinman, N. Turro, D. Krantz, RH Edwards, LA. Greene and L. Zecca, "Neuromelanin Biosynthesis is Driven by Excess Cytosolic Catecholamines Not Accumulated by Synaptic Vesicles", *Proc Natl Acad Sci U S A*, 97(22),11869–11874 (2000).
8. W. Jin, S.J. Stehbins, R. T. Barnard, M. A. Blaskovich and Z. M. Ziora, "Dysregulation of tyrosinase activity: a potential link between skin disorders and neurodegeneration", *JPP*, 76(1),13-22 (2024).
9. Q. Li, J. Mo, B. Xiong, Q. Liao, Y. Chen, Y. Wang, S. Xing, S. He, W. Lyu, N. Zhang and H. Sun, "Discovery of resorcinol-based polycyclic structures as tyrosinase inhibitors for treatment of Parkinson's disease", *ACS Chem Neurosci*, 13(1), 81-96(2021).
10. G. Luisi, A. Stefanucci, G. Zengin, M. P. Dimmito and A. Mollica, "Anti-oxidant and tyrosinase inhibitory in vitro activity of amino acids and small peptides: New hints for the multifaceted treatment of neurologic and metabolic disfunctions", *Antioxidants (Basel)*, 8(1),7 (2018).
11. D. P. Jones, "Redefining oxidative stress", *Antioxid Redox Signal*, 8(9-10),1865-1798 (2006).
12. D. Sergi, H. Boulestin, F.M. Campbell and L.M. Williams, "The role of dietary advanced glycation end products in metabolic dysfunction", *Mol Nutr Food Res*, 65(1), e1900934 (2021) .
13. W. Rungratanawanich, Y. Qu, X. Wang, M. M. Essa and B. J. Song "Advanced glycation end products (AGEs) and other adducts in aging-related diseases and alcoholmediated tissue injury", *Exp Mol Med*, 53(2), 168–188 (2021).
14. M. Szeliga, "Peroxiredoxins in neurodegenerative diseases", *Antioxidants*, 9(12),1203 (2020).
15. M. Szeliga, "Peroxiredoxins in neurodegenerative diseases", *Antioxidants*, 9(12),1203 (2020).
16. J.P. Declercq, C. Evrard, A. Clippe, D. Vander Stricht, A. Bernard and B. Knoop, "Crystal structure of human peroxiredoxin 5, a novel type of mammalian peroxiredoxin at 1.5 Å resolution", *J Mol Biol*, 311(4),751-759 (2001).
17. J.P. James, V. Devaraji, P. Sasidharan and T.S Pavan, " Pharmacophore Modeling, 3D QSAR, Molecular Dynamics Studies and Virtual Screening on Pyrazolopyrimidines as anti-Breast Cancer Agents", *PACs*, 43(8),7456-7473 (2023).
18. J. P. James, P. Sasidharan, S. P. Mandal and S. R. Dixit, "Virtual Screening of Alkaloids and Flavonoids as Acetylcholinesterase and MAO-B Inhibitors by Molecular Docking and Dynamic Simulation Studies", *PACs*, 43(6),5453-5477 (2023).
19. T. Qadir, A. Amin, P. K. Sharma, I. Jeelani and H. Abe, "A review on medicinally important heterocyclic compounds", *Open J Med Chem*,16(1), (2022).
20. Y. Li, J. Geng, Y. Liu, S. Yu and G. Zhao, "Thiadiazole—A promising structure in medicinal chemistry", *ChemMedChem*, 8(1), 27-41 (2013).
21. U. A. Atmaram and S. M. Roopan,

- "Biological activity of oxadiazole and thiadiazole derivatives", *Appl Microbiol Biotechnol*, 106(9),3489- 505(2022).
22. F. Begum, M. Yousaf, S. Iqbal, N. Ullah, A. Hussain, M. Khan, A. Khalid, A. S. Algarni, A.N. Abdalla, A. Khan and M. A. Lodhi, "Inhibition of Acetylcholinesterase with Novel 1, 3, 4, Oxadiazole Derivatives: A Kinetic, In Silico, and In Vitro Approach", *ACS Omega*, 8(49),46816-29 (2023).
 23. B. A. Khan, S. S. Hamdani, S. Jalil, S. A. Ejaz, J. Iqbal, A.M. Shawky, A. M. Alqahtani, G. A. Gabr, M. A. Ibrahim and P. A. Sidhom, "Synthesis and evaluation of novel S-alkyl phthalimide-and S-benzyl-oxadiazole-quinoline hybrids as inhibitors of monoamine oxidase and acetylcholinesterase" , *Pharmaceuticals*, 22,16(1),11 (2022).
 24. M. Hatami, Z. Basri, B. K. Sakhvidi and M. Mortazavi, "Thiadiazole–A promising structure in design and development of anti-Alzheimer agents", *Int Immunopharmacol*, 118(16),110027 (2023).
 25. J. F. González, A. R. Alcántara, A. L. Doadrio and J. M. Sánchez-Montero, "Developments with multi-target drugs for Alzheimer's disease: An overview of the current discovery approaches", *Expert Opin Drug Discov*, 14(9), 879-891 (2019).
 26. O. Gerlits, K. Y. Ho, X. Cheng, D. Blumenthal, P. Taylor, A. Kovalevsky and Z. Radić, "A new crystal form of human acetylcholinesterase for exploratory room-temperature crystallography studie", *Chem Biol Interact*, 309,108698 (2019).
 27. B. Deri, M. Kanteev, M. Goldfeder, D. Lecina, V. Guallar, N. Adir and A. Fishman, "The unravelling of the complex pattern of tyrosinase inhibition", *Scien Rep*, 6(1), 1-10 (2016).
 28. J. P. Declercq, C. Evrard, A. Clippe, D. V. Stricht, A. Bernard and B. Knoops, "Crystal structure of human peroxiredoxin 5, a novel type of mammalian peroxiredoxin at 1.5 Å resolution", *J Mol Biol*, 311(4),751-759 (2001).
 29. J. P. James, T.C. Aiswarya, S. N. Priya, D. I. Jyothi, S. R. Dixit, "Structure based multitargeted molecular docking analysis of pyrazole-condensed heterocyclics against lung cancer", *Int J App Pharm*,3(6),157-169 (2021).
 30. L. Dong, X. Qu, Y. Zhao and B. Wang, "Prediction of binding free energy of protein–ligand complexes with a hybrid molecular mechanics/generalized born surface area and machine learning method", *ACS Omega*, 6(48), 32938-32947 (2021).
 31. J.P. James, P. D. Ail, L. Crasta, R.S. Kamath, M.H. Shura and T.J. Sindhu, "In silico ADMET and molecular interaction profiles of phytochemicals from medicinal plants in Dakshina Kannada", *JHAS*, 14(02),190-201 (2024).
 32. F. Ntie-Kang, J.A. Mbah, L.L. Lifongo, L.C. Owono Owono, E. Megnassan, L. Meva'a Mbaze, P.N. Judson, W. Sippl and S.M. Efange, "Assessing the pharmacokinetic profile of the CamMedNP natural products database: an in silico approach", *Bioorg Med Chem Lett*, 3, 1-9 (2013).
 33. M.S. Chande, M.A. Pankhi and S.B. Ambhaikar, "Synthesis of new heterocycles by using thiocarbohydrazide and thiosemicarbazides", *NOPR*, 39(8), 603-609 (2000).
 34. M. H. Shih and C.L. Wu, "Efficient syntheses of thiadiazoline and thiadiazole derivatives by the cyclization of 3-aryl-4-formylsydnone thiosemicarbazones with acetic anhydride and ferric chloride", *Tetrahedron*, 61(46), 10917-10925 (2005).
 35. C. Mohan, V. Kumar, N. Kumari, S. Kumari, J. Yadav, T. Gandass and S. Yadav, "Synthesis, characterization and antibacterial activity of semicarbazide based Schiff bases and their Pb (II), Zr (IV) and U (VI) complexes", *Adv J Chem*, 2,187-96 (2020).
 36. D. T. Nguyen, T. H. Le and T. T. Bui, "Antioxidant activities of thiosemicarbazones from substituted benzaldehydes and N-(tetra-O-acetyl-β-D-galactopyranosyl) thiosemicarbazide", *Eur J Med Chem*, 60, 199-207 (2013).
 37. U. Košak, N. Strašek, D. Knez, M. Jukič, S. Žakelj, A. Zahirović, A. Pišlar, X. Brazzolotto, F. Nachon, J. Kos and S. Gobec, "N-alkylpiperidine carbamates as potential anti-Alzheimer's agents", *Eur J Med Chem*, 197, 112282 (2020).
 38. H. X. Cui, F. F. Duan, S. S. Jia, F. R. Cheng and K. Yuan, "Antioxidant and Tyrosinase Inhibitory Activities of Seed

- Oils from *Torreya grandis* Fort. ex Lindl.", *Biomed Res Int*, 2018(1),5314320 (2018).
39. M. Ashooriha, M. Khoshneviszadeh, A. Rafiei, M. Kardan, R. Yazdian-Robati and S. Emami, "Kojic acid–natural product conjugates as mushroom tyrosinase inhibitors", *Eur J Med Chem*, 201,112480 (2020).
 40. S. Keser, S. Celik, S. Turkoglu, O. Yilmaz and I. Turkoglu, "Hydrogen peroxide radical scavenging and total antioxidant activity of hawthorn", *Chem J*, 2(1), 9-12 (2012).
 41. S. S. Ahmad, M. B. Khan, K. Ahmad, J. H. Lim, S. Shaikh, E. J. Lee and I. Choi, "Biocomputational screening of natural compounds against acetylcholinesterase", *Molecules*, 26(9), 2641 (2021).
 42. M. Taha, F. Rahim, N. Uddin, I. U. Khan, N. Iqbal, M. Salahuddin, R. K. Farooq, M. Gollapalli, K. M. Khan and A. Zafar, "Exploring indole-based-thiadiazole derivatives as potent acetylcholinesterase and butyrylcholinesterase enzyme inhibitors", *Int J Biol Macromol*, 188,1025-36 (2021).
 43. K. N. Alcorn, I. A. Oberhauser, M. D. Politeski and T. J. Eckroat, "Evaluation of N-alkyl isatins and indoles as acetylcholinesterase and butyrylcholinesterase inhibitors", *J Enzyme Inhib Med Chem*, 39(1), 2286935 (2024).
 44. A. Hiremathad and L. Piemontese, "Heterocyclic compounds as key structures for the interaction with old and new targets in Alzheimer's disease therapy", *Neural Regen Res*, 12(8),1256-61 (2017).



نشرة العلوم الصيدلانية جامعة أسيوط



دراسات النشاط المثبط لإنزيم أستيل كولينستراز والتيروزيناز والبيروكسيريديوكسين للأوكساديازول والثياديازول المركب من قواعد شيف

كيرثان - سيندهوت. ج - جيني ب. جيمس* - زكية فاطيما

قسم الكيمياء الصيدلانية، جامعة نيت، معهد NGSM للعلوم الصيدلانية (NGSMIPS)، ديراالكات، مانجالورو

٥٢٥٠١٨، كارناتاكا، الهند

مع تزايد انتشار الأمراض التنكسية العصبية (NDDs) والفعالية المحدودة للعلاجات الحالية، هناك حاجة ملحة لاكتشاف خيوط علاجية جديدة يمكن أن تتفاعل مع أهداف متعددة تتسبب في NDD. تم تصميم سلسلة جديدة من مشتقات ١،٣،٤-أوكساديازول-٢-أمينو ١،٣،٤-ثياديازول-٢-أمين لتقييم الإمكانيات المثبطة لهذه المركبات ضد أستيل كولينستراز، تم اختبار التيروزيناز والبيروكسيريديوكسينات باستخدام طرق السيليكو وفي المختبر. تم تصنيع مشتقات أوكساديازول (٤ أ، ٤ د) وثياديازول (٤ هـ، ٤ ج، ٤ ساعات) عن طريق تدوير قاعدة شيف باستخدام $FeCl_3$ ، تم تقييمها ب FTIR و $^1H NMR$ وأطياف الكتلة. تم تقييم أستيل كولينستراز، التيروزيناز وإنزيمات البيروكسيريديوكسين في الدراسات المثبطة في المختبر. كشف الالتحام الجزيئي أن المركبات a_4 و e_4 تتفاعل بشكل فعال ضد أستيل كولينستراز وتيروزيناز. أظهرت النتائج في المختبر أن المركبات a_4 و e_4 أظهرت أعلى نشاط مثبط ضد أستيل كولينستراز والتيروزيناز وكانت عوامل مضادة للأكسدة جيدة.

أكدت نتائج الالتحام المرتبطة بالنتائج في المختبر أن المركب a_4 من سلسلة أوكساديازول والمركب e_4 من سلسلة ثياديازول كان له أقوى نشاط مثبط للأستيل كولينستراز والتيروزيناز. أظهرت نتائج التحليل أن المجموعات الحلقية غير المتجانسة قد تكون سببا لتحسين عمل أستيل كولينستراز ومثبطات التيروزيناز. يشير هذا إلى مجال إضافي لاستكشاف هذه المشتقات بشكل أكبر كعامل وقائي للأعصاب لفهم أفضل للآليات الأساسية والفيزيولوجيا المرضية.